

論文 / 著書情報
Article / Book Information

| | |
|-----------|---|
| Title | Data augmentation in EUV lithography simulation based on convolutional neural network |
| Authors | Hiroyoshi Tanabe, Atsushi Takahashi |
| Citation | , , , |
| Pub. date | 2022, 5 |
| DOI | https://doi.org/10.1117/12.2615267 |
| Rights | <p>(Copyright) Copyright 2022 Society of Photo Optical Instrumentation Engineers (SPIE). One print or electronic copy may be made for personal use only. Systematic reproduction and distribution, duplication of any material in this publication for a fee or for commercial purposes, and modification of the contents of the publication are prohibited.</p> <p>(Citation) Hiroyoshi Tanabe, Atsushi Takahashi "Data augmentation in EUV lithography simulation based on convolutional neural network", Proc. SPIE 12052, DTCO and Computational Patterning, 120520T (26 May 2022); https://doi.org/10.1117/12.2615267</p> |

PROCEEDINGS OF SPIE

SPIDigitalLibrary.org/conference-proceedings-of-spie

Data augmentation in EUV lithography simulation based on convolutional neural network

Hiroyoshi Tanabe, Atsushi Takahashi

Hiroyoshi Tanabe, Atsushi Takahashi, "Data augmentation in EUV lithography simulation based on convolutional neural network," Proc. SPIE 12052, DTCO and Computational Patterning, 120520T (26 May 2022); doi: 10.1117/12.2615267

SPIE.

Event: SPIE Advanced Lithography + Patterning, 2022, San Jose, California, United States

Data augmentation in EUV lithography simulation based on convolutional neural network

Hiroyoshi Tanabe and Atsushi Takahashi

Tokyo Institute of Technology, 2-12-1 Ookayama, Meguro-ku, Tokyo 152-8550 Japan

ABSTRACT

Data augmentation is a powerful technique in deep learning to increase the number of training data by using limited original data. We apply this technique to EUV lithography simulation based on convolutional neural network (CNN). In previous work, we developed a prototype CNN which reproduces the results of the rigorous electromagnetic (EM) simulations in a small mask area. The prediction time of CNN was 5,000 times faster than the calculation time of EM simulation. We trained the CNN by using 200,000 data which were the results of EM simulation. Although the prediction time of CNN was very short, it took a long time to build a huge amount of the training data. Especially when we enlarge the mask area the calculation time to prepare the training data becomes unacceptably long. The EM calculation time for 1,024 nm X 1,024 nm mask area takes 162 s. It will take a year to calculate 200,000 mask patterns. The training data of our CNN is the diffraction amplitudes of mask patterns. Assuming a periodic boundary condition, the diffraction amplitudes of the shifted or flipped mask pattern can be easily calculated by using the diffraction amplitudes of the original mask pattern. We apply this data augmentation technique to reduce the data preparation time for 1,024 nm X 1,024 nm mask area by a factor of 200. The accuracy of CNN is verified by comparing the CNN predictions with the results of EM simulation. Our CNN successfully reproduces critical dimensions and edge placement errors of line and space patterns.

Keywords: lithography simulation, neural network, EUV mask

1. INTRODUCTION

High aspect absorbers used in extremely ultraviolet (EUV) masks induce several mask 3D effects such as critical dimension (CD) and image placement errors.^{1,2} It is necessary to include the mask 3D effects in EUV lithography simulation. Mask 3D effects can be calculated rigorously by using electromagnetic (EM) simulators.³⁻⁵ However, these simulators are highly time consuming for full-chip applications.

Recently, many attempts have been made to simulate the mask 3D effects by using deep neural networks (DNNs). They are classified into three models depending on the targets of DNNs. Three possible targets are, from the mask to the wafer, the near-field amplitude on the mask, the far-field amplitude (diffraction spectrum) at the pupil of the projection optics, and the image intensity on the wafer. In the first model the target is the near-field amplitude on the mask calculated by electromagnetic simulation.⁶⁻⁹ One of the difficulties in this model is that many DNNs are required to reproduce different near-field amplitudes depending on the source position. In the second model, which is our model,¹⁰ the target of DNN is the far-field amplitude at the pupil of the projection optics. Since the far-field amplitudes are described in frequency space, our model naturally parametrizes the source position dependence of the amplitude. The third model^{11,12} uses the image intensity on the wafer as the target of DNN. This model is much straightforward than other models because the image intensity is used in the following resist simulation. However, the phase information is lost when the diffraction amplitude is converted to the image intensity. Mask 3D effects depend on the phase of the amplitude, but it is not directly included in the model. Further study is needed to see if the model can reproduce various aspects of the mask 3D effects.

In our previous work,¹⁰ we developed a prototype convolutional neural network (CNN) which reproduces the results of the rigorous EM simulation in a small mask area. The prediction time of CNN was 5,000 times faster than the calculation time of EM simulation. We trained the CNN by using 200,000 data which were the results of EM simulation. Such a large amount of the data was necessary to reduce the validation loss after the training. Although the prediction time of CNN was very short, it took a long time to build the training data. Creating the training data in the work was possible because the mask area was small. However, when we enlarge the mask area for practical applications the calculation time to prepare the training data becomes unacceptably long.

In this work, we apply data augmentation technique to our CNN, which is standard in DNN. We increase the number of the training data without performing EM calculation, which significantly reduces the time to prepare the training data. In Sec. 2, we explain the detail of our data augmentation technique. In Sec. 3, we study the accuracy of our CNN prediction on critical dimensions and edge placement errors. Sec. 4 is the summary.

2. DATA AUGMENTATION FOR LARGE MASK PATTERNS

In the previous work¹⁰ we assumed a periodic mask pattern with 720 nm X 720 nm mask area. We should not use the edges of the mask area to avoid the influence of the neighboring mask pattern. According to Ref. 13, the optical interaction range R_{opt} is calculated by the following equation.

$$R_{opt} = \frac{1.12\lambda}{\sigma NA}, \quad (1)$$

where λ , σ , and NA represent the wavelength, coherence factor, and numerical aperture of the scanner, respectively. The wavelength of EUV light is 13.5 nm and the numerical aperture of the current EUV scanner is 0.33. The coherence factor depends on the illumination setting and the typical value is 0.5. Insetting these values in Eq. 1, the optical interaction range $R_{opt} = 90$ nm. This value is the size on the wafer, and the number is multiplied by four on the mask. Therefore, the optical interaction range on the mask is $4 \times R_{opt} = 360$ nm. Figure 1 shows the usable mask area excluding the area influenced by the neighboring mask pattern. The mask size L should be larger than 720 nm to get the usable mask area. Therefore, there was no usable area in the previous work.

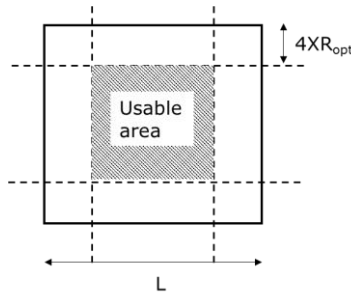


Fig. 1 Usable mask area

In this work we choose 1,024 nm X 1,024 nm mask area. The usable mask area is 300 nm square. The usable area is not large, but the EM calculation time highly depends on the size of the mask area. The calculation time of 1,024 nm X 1,024 nm mask area takes 162 s by using Core i9-9900K CPU. Deep neural networks require a large amount of the training data. In the previous work we used 200,000 training data. It will take a year if we calculate the same number of the data with the mask area in this work.

Data augmentation is a powerful technique in deep learning to increase the number of the training data with limited original data. In our CNN the input is the mask pattern, and the outputs are the far-field diffraction amplitude $A(l, m; l_s, m_s)$, where (l, m) is the diffraction order and (l_s, m_s) is the source position. When the mask pattern is shifted or Y-flipped as shown in Fig. 2, the diffraction amplitudes of these patterns can be easily calculated from that of the original pattern. Note that in EUV reflective optics, X-flip is not symmetrical to the chief ray because it is tilted 6 degrees in Y direction.

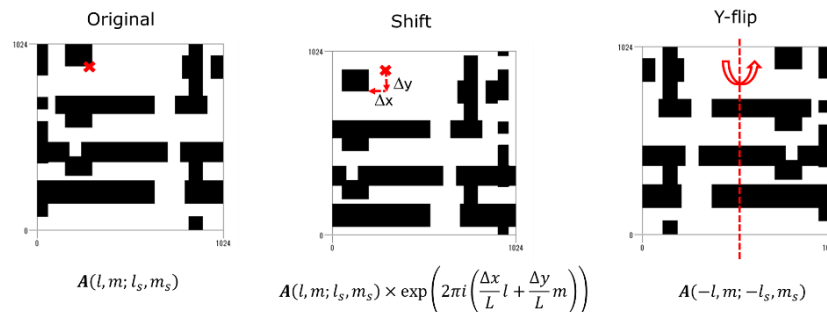


Fig. 2 Original, shifted and Y-flipped mask patterns.

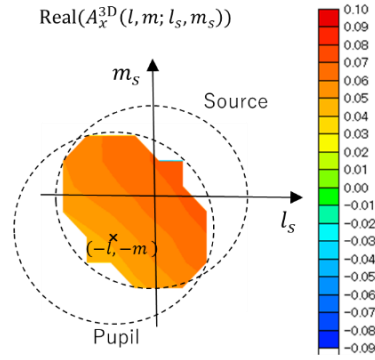


Fig.3 Source position dependence of the mask 3D amplitude

Following Ref. 10 the far-field diffraction amplitude $A(l, m; l_s, m_s)$ is divided into the thin mask amplitude (Fourier transform of the mask pattern) $A^{FT}(l, m)$ and the mask 3D amplitude $A^{3D}(l, m; l_s, m_s)$.

$$A(l, m; l_s, m_s) = A^{FT}(l, m) + A^{3D}(l, m; l_s, m_s). \quad (2)$$

Figure 3 shows the source position dependence of the mask 3D amplitude. The source position where the amplitude contributes to the image intensity is limited by the source shape and the pupil shape. Only the overlapping area in Fig.3 contributes to the intensity. We approximate the mask 3D amplitude in this area by a linear function of the source position as follows.

$$A_x^{3D}(l, m; l_s, m_s) \cong a_0(l, m) + a_x(l, m) (l_s + l/2) + a_y(l, m) (m_s + m/2), \quad (3)$$

where a_0 is the mask 3D amplitude at the center of the overlapping area, $(l_s, m_s) = (-l/2, -m/2)$, and a_x and a_y are the slopes of the amplitude in the x and y directions on the source plane, respectively. We call these three numbers as mask 3D parameters.

The values of mask 3D parameters are determined by the mask pattern and the absorber. We construct CNN to predict the mask 3D parameters from the mask pattern. We assume Ta absorber with 50 nm thickness. Figure 4 shows the architecture of our CNN. Three independent CNNs are used for three mask 3D parameters. The input is a random line or space pattern with a mask area of 1,024 nm X 1,024 nm. 1,024X1,024 binary data is averaged to 128X128 float data before inputting to the CNNs. Circular padding¹⁴ is used in CNNs because we assume periodic boundary conditions for input mask patterns.

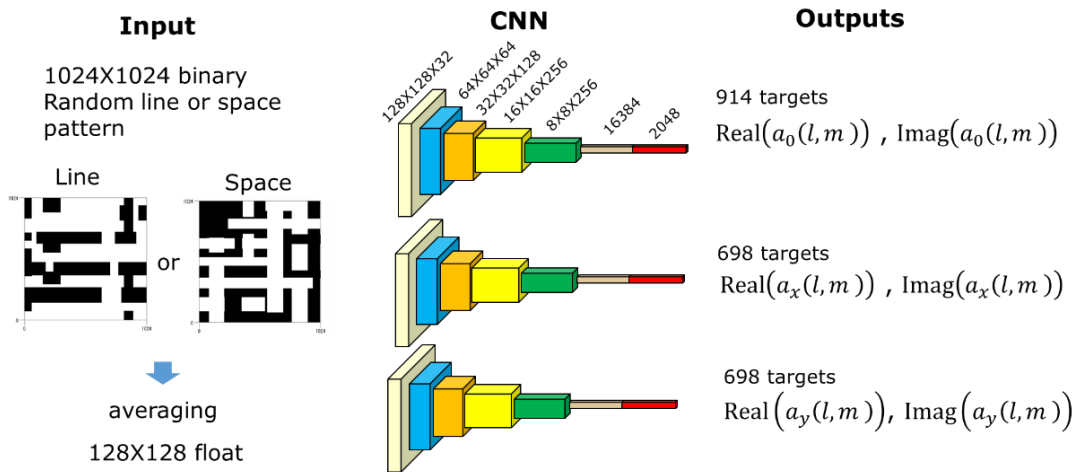
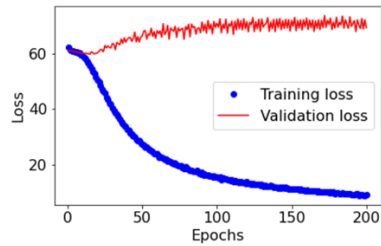


Fig. 4 Architecture of our CNN.

Without data augmentation

of training data: 2,500 (original)
of validation data: 1,000 (original)



With data augmentation

of training data: 500,000
= 2,500 (original) X 200 (data augmentation)
of validation data: 1,000 (original)

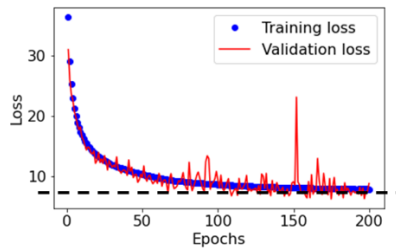


Fig. 5 Loss functions of training and validation data with/without data augmentation.

Figure 5 shows the loss functions of training and validation data. The number of the original data for training is 2,500 and the number of the data for validation is 1,000. With data augmentation, the original data is shifted by 100 nm pitch in both X and Y directions and flipped along the Y axis. Therefore, the number of the training data after the data augmentation is multiplied by 200 to 500,000.

Without data augmentation the training loss decreases after the training while the validation loss does not. This is a typical overfitting phenomenon in DNN. With data augmentation both the training loss and the validation loss decrease after the training. However, even with data augmentation, the validation loss does not approach to zero. This may mean the insufficient capability of our CNN architecture.

3. CNN PREDICTION ACCURACY

After the training we study the accuracy of our CNN. Figure 6 compares the mask 3D parameters at several diffraction orders. The correlation between the parameters by EM simulation and CNN predictions is moderately good. The correlation of $\text{Real}(a_x(0,0))$ is poor but the value is very small compared to the values of other parameters.

The accuracy of our CNN is verified by calculating the image intensities of test mask patterns. Figure 7 compares the image intensities of a line mask pattern by EM simulation, Fourier Transformation (FT) and CNN prediction. As mentioned

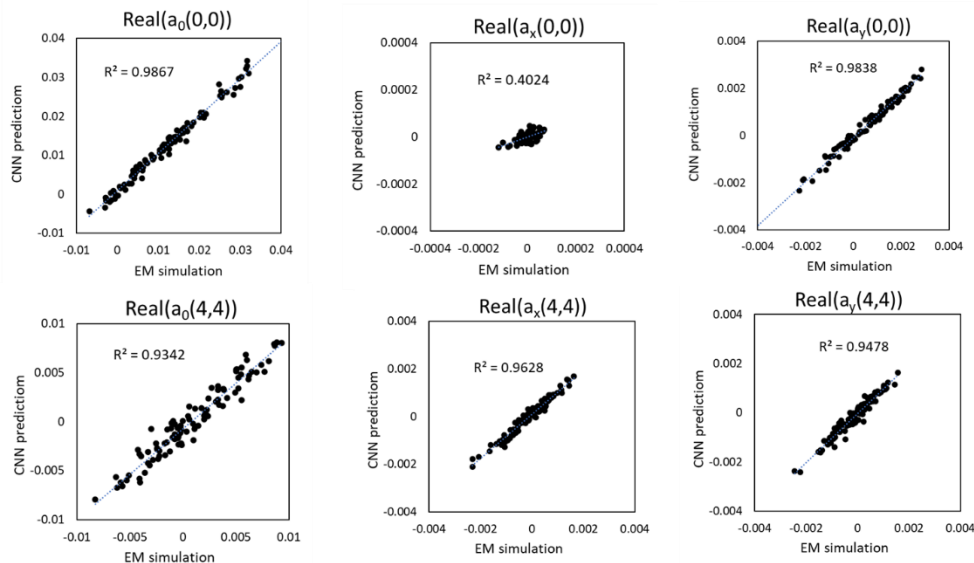


Fig. 6 Mask 3D parameters calculated by EM simulations and parameters predicted by CNN.

in the previous section, the wavelength is 13.5 nm and NA is 0.33. We assume annular illumination with $\sigma_{in}/\sigma_{out}=0.3/0.8$. The bottom figures show the difference of the intensities between EM simulation and FT or CNN prediction. The difference between EM and CNN is much smaller than the difference between FT and EM. Figure 8 compares the critical dimension (CDs) and the edge placement errors (EPEs) of vertical (V) lines and horizontal (H) lines with several line width. The agreement between EM simulation and CNN prediction is good though small errors remain.

Figure 9 compares the image intensities of a space mask pattern and Fig. 10 shows the CDs and EPEs of V and H spaces with several space width. Similar results can be seen with space patterns as with line patterns.

4. SUMMARY

Data augmentation technique was applied to the diffraction amplitude of the mask pattern. Diffraction amplitudes of shifted or Y-flipped mask patterns were calculated by using the diffraction amplitude of the original mask pattern. The number of the training data after the data augmentation is multiplied by 200 from 2,500 to 500,000. Large number of the training data was required to reduce the validation loss of CNN.

Even with the data augmentation, the validation loss did not approach to zero. Our CNN almost reproduced the CDs and EPEs of line and space patterns, but small errors remained. Although the errors are small, higher accuracy is desired for practical applications.

We expanded the mask area from the previous work to get the usable area of 300 nm square on the mask. The usable area is still small. Our CNN architecture needs improvement. It is a challenge to develop CNN for larger mask area and more general patterns with higher accuracy.

REFERENCES

- [1] V. Philipsen, "Mask is key to unlock full EUV potential," Proc. SPIE 11609(2021).
- [2] A. Erdmann, P. Evanschitzky, G. Bottiglieri, E. Setten and T. Fliervoet, "3D mask effects in high NA EUV imaging," Proc. SPIE 10957, 109570Z (2019).
- [3] A. Wong, "TEMPEST users' guide", UCB/ERL M94/64 (1994).
- [4] M.G. Moharam and T.K. Gaylord, "Rigorous coupled-wave analysis of planar-grating diffraction," J. Opt. Soc. Am. 71(1981) 811.
- [5] K.D. Lucas, H. Tanabe and A.J. Strojwas, "Efficient and rigorous three-dimensional model for optical lithography simulation," J. Opt. Soc. Am. A 13(1996)2187.
- [6] S. Lan, J. Liu, Y. Wang, K. Zhao and J. Li, "Deep learning assisted fast mask optimization," Proc. SPIE 10587 (2018)105870H.
- [7] P. Liu, "Mask synthesis using machine learning software and hardware platforms," Proc. SPIE 11327 (2020)1132707.
- [8] R. Pearman, M. Meyer, J. Ungar, H. Yu, L. Pang and A. Fujimura, "Fast all-angle mask 3D ILT patterning," Proc. SPIE 11327 (2020)113270F.
- [9] J. Lin, L. Dong, T. Fan, X. Ma, R. Chen and Y. Wei, "Fast mask near-field calculation using fully convolution network," International Workshop Adv. Patterning Solutions (2020).
- [10] H. Tanabe, S. Sato and A. Takahashi, "Fast EUV lithography simulation using convolutional neural network," J. Micro/Nanopattern. Mater. Metrol. 041202 (2021).
- [11] W. Ye, M.B. Alawieh, Y. Watanabe, S. Nojima, Y. Lin and D.Z. Pan, "TEMPO: fast mask topography effect modeling with deep learning," Int. Symp. Phys. Design '20, (2020)127.
- [12] A. Awad, P. Brendel, P. Evanschitzky, D.S. Woleamanual, A. Roskopf and A. Erdmann, "Accurate prediction of EUV lithographic images and 3D mask effects using generative networks," J. Micro/Nanopattern. Mater. Metrol. 043201 (2021).
- [13] A. Wong, "Resolution enhancement techniques in optical lithography," SPIE Press (2001).
- [14] S. Schubert, P. Neubert, J. Poeschmann and P. Protzel, "Circular convolutional neural networks for panoramic images and laser data," Proc. IEEE Intelligent Vehicle Symposium (IV) (2019).

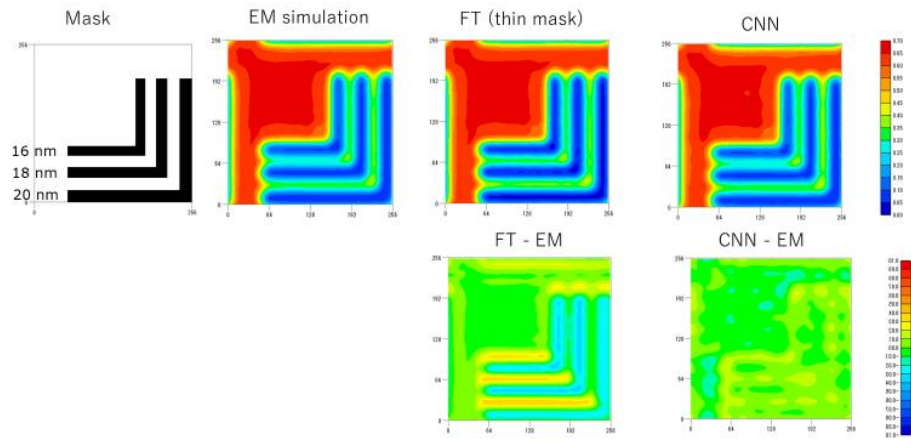


Fig. 7 Line mask pattern and its image intensities by EM simulation, Fourier Transformation and CNN prediction.

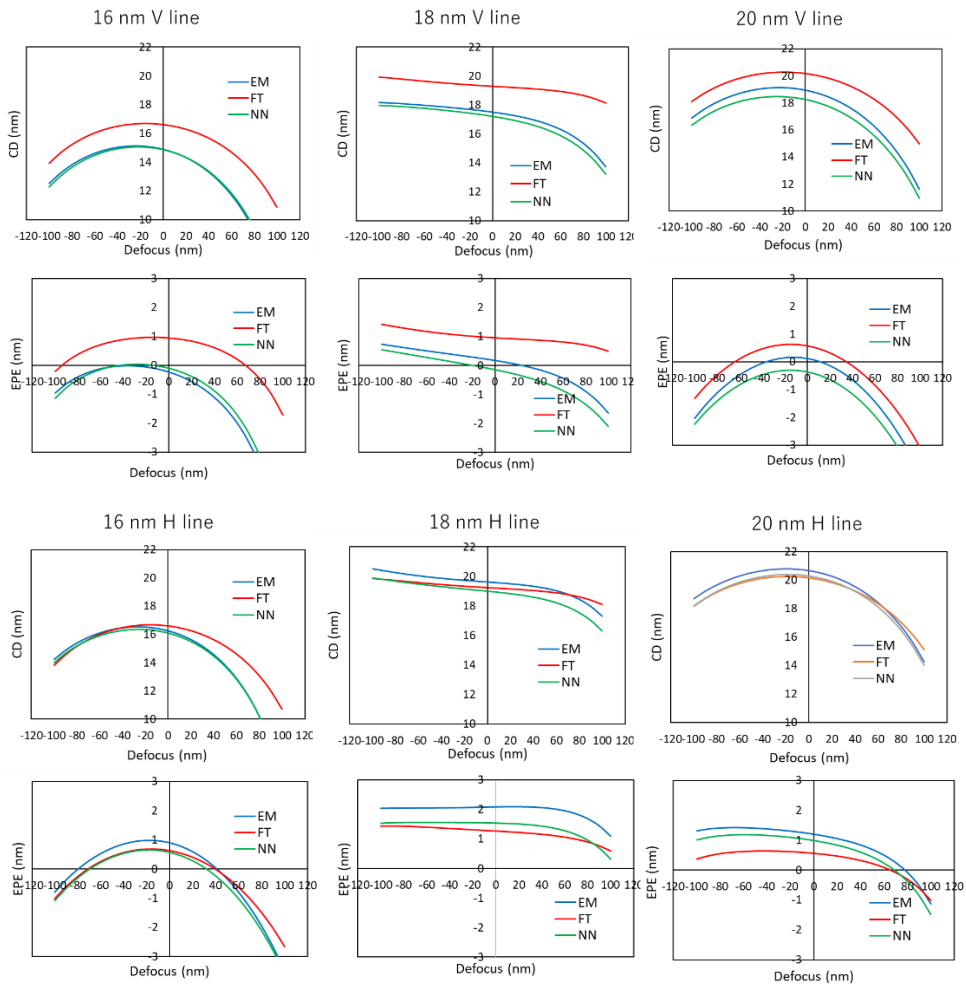


Fig. 8 CDs and EPEs of vertical and horizontal lines.

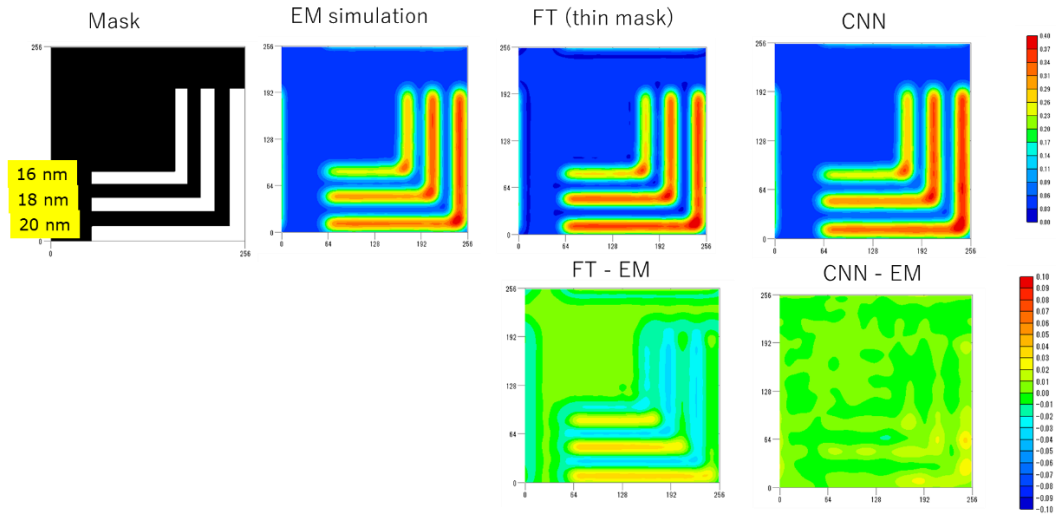


Fig. 9 Space mask pattern and its image intensities by EM simulation, Fourier Transformation and CNN prediction.

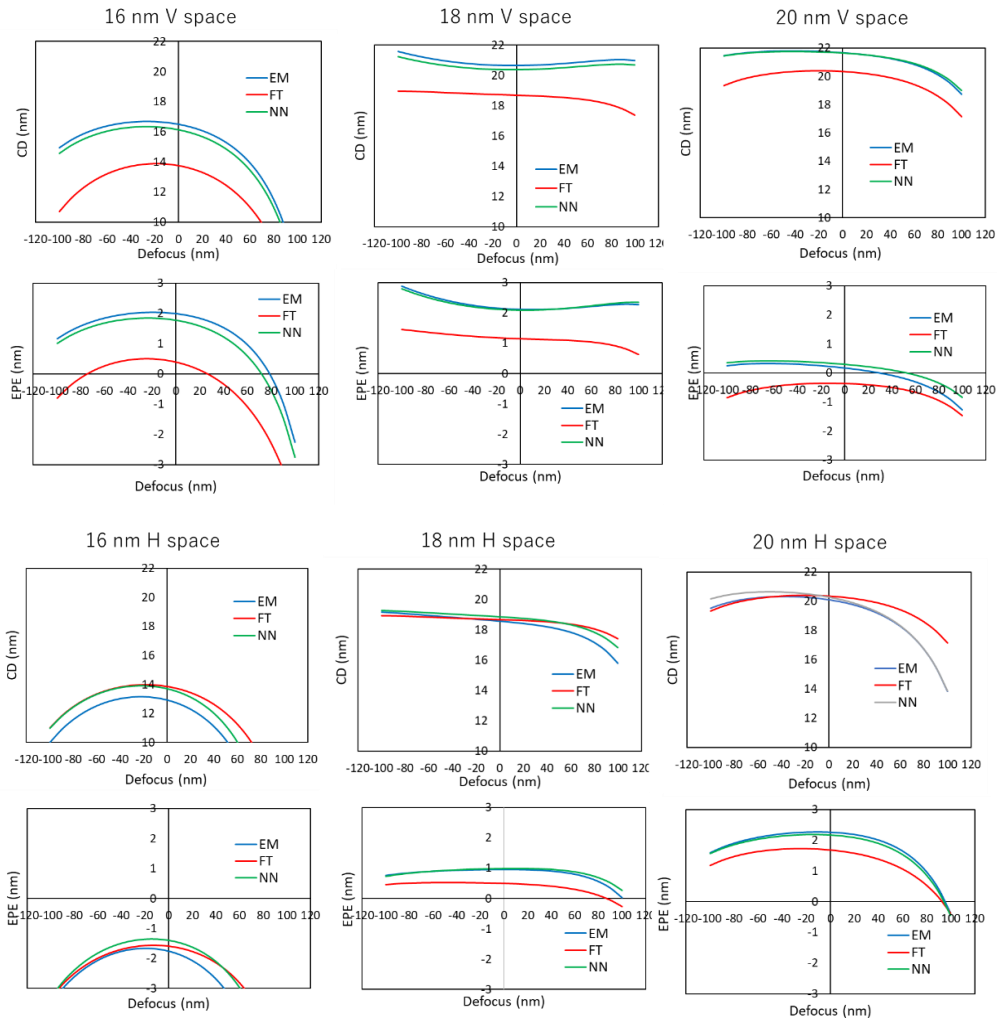


Fig. 10 CDs and EPEs of vertical and horizontal spaces.